PHYSICAL REVIEW A **93**, 031403(R) (2016)

Atomic photoionization experiment by harmonic-generation spectroscopy

M. V. Frolov,[1,2] T. S. Sarantseva,[2] N. L. Manakov,[1] K. D. Fulfer,[3] B. P. Wilson,[3] J. Troß,[4,5] X. Ren,[4,6] E. D. Poliakoff,[3] A. A. Silaev,[2] N. V. Vvedenskii,[2] Anthony F. Starace,[7] and C. A. Trallero-Herrero[4]

[1]*Department of Physics, Voronezh State University, Voronezh 394006, Russia*

[2]*Institute of Applied Physics, Russian Academy of Sciences, Nizhny Novgorod 603950, Russia*

[3]*Department of Chemistry, Louisiana State University, Baton Rouge, Louisiana 70803, USA*

[4]*J. R. Macdonald Laboratory, Kansas State University, Manhattan, Kansas 66506-2604, USA*

[5]*Institut für Kernphysik, Goethe Universität, Max-von-Laue-Strasse 1, 60438 Frankfurt am Main, Germany*

[6]*Institute for the Frontier of Attosecond Science and Technology, CREOL, and Department of Physics, University of Central Florida, Orlando, Florida 32816-2385, USA*

[7]*Department of Physics and Astronomy, University of Nebraska, Lincoln, Nebraska 68588-0299, USA*

(Received 26 August 2015; published 17 March 2016)

Measurements of the high-order-harmonic generation yield of the argon (Ar) atom driven by a strong elliptically polarized laser field are shown to completely determine the field-free differential photoionization cross section of Ar, i.e., the energy dependence of both the angle-integrated photoionization cross section and the angular distribution asymmetry parameter.

DOI: 10.1103/PhysRevA.93.031403

Advances in laser technologies have enabled measurements of atoms and molecules that provide detailed views of their structures as well as the ability to image ultrafast processes on attosecond (10^{-18} s) time scales [1–6]. Nevertheless, the most common method for obtaining information on the electronic structure of atoms and molecules remains single-photon ionization (since the photoelectron angular and energy distributions are sensitive to both the initial target wave function and the final-state wave function of the ion and continuum electron [7–9]). Photoionization experiments nowadays are typically carried out at synchrotron or free-electron laser light source facilities. An appeal of laser spectroscopy for photoionization measurements is the tabletop size of the experimental setup. However, a main obstacle for laser spectroscopy measurements of energy-resolved photoionization spectra is the need for tunable laser sources. This remains a challenge in the important VUV and XUV photon energy regions. However, this problem can be overcome by high-order-harmonic generation (HHG) spectroscopy [10–14], which permits fully coherent, energy-resolved photoionization measurements with a laser field whose frequency is much smaller than the ionization potentials of typical atomic or molecular targets. This connection of the nonlinear harmonic-generation process with the linear photoionization process is one of the key advances in our understanding of strong-field processes.

HHG spectroscopy is based on the quasiclassical interpretation of HHG as a three-step process [3,15,16]: (i) tunnel ionization of an electron in an atomic or molecular target by a strong low-frequency laser field; (ii) propagation of the ionized electron in the laser-dressed continuum away from and back to the target ion by the oscillating field; and (iii) recombination of the returning electron back to the target ground state with emission of a harmonic photon. The intensity of the harmonic radiation carries information on the photorecombination cross section (PRCS), which is related (through the principle of detailed balance) to that for photoionization. The retrieval of the PRCS is based on the phenomenological parametrization of the HHG yield Y as the product of an electronic wave packet $W(E)$ and the field-free PRCS $\sigma(E)$ [17,18],

$$Y \propto W(E)\sigma(E), \quad E = E_\Omega - I_p, \tag{1}$$

where E is the energy of the recombining electron, E_Ω is the harmonic energy, and I_p is the target binding energy. The parametrization (1) is valid in the tunneling regime and involves the *exact* PRCS for an electron having momentum directed along the polarization axis of the linearly polarized harmonic photon [19]. It has been confirmed in recent HHG experiments [10–14] and theoretical analyses [20,21] involving linearly polarized driving laser fields. These investigations all demonstrate that HHG spectra reveal structure-dependent target details. However, none retrieves completely the PRCS (or photoionization cross section), which (in the electric dipole approximation and for an unpolarized target) may be expressed in terms of two parameters [7–9]: the total cross section $\sigma_0(E)$ and the asymmetry parameter $\beta(E)$,

$$\sigma(E,\theta) = \frac{\sigma_0(E)}{4\pi}\left[1 + \frac{\beta(E)}{2}(3\cos^2\theta - 1)\right], \tag{2}$$

where θ is the angle between the polarization vector of the emitted (or absorbed) linearly polarized photon and the momentum of the recombining (or ionized) electron. Since the HHG yield (1) includes only the cross section $\sigma(E) = \sigma(E,\theta = 0^\circ)$, HHG with a linearly polarized field does not allow the retrieval of the two independent parameters, $\sigma_0(E)$ and $\beta(E)$, which completely describe also the photoionization cross section of an atom in an elliptically polarized field [22–24]. Procedures for retrieving σ_0 and β by means of HHG spectroscopy have been derived theoretically [25,26]. However, their requirements for either precise harmonic polarization measurements [25] or stabilization of the relative phase of a two-color field [26] present challenges for experiment.

In this Rapid Communication we show that the parameters σ_0 and β can be retrieved from measurements of high-order-harmonic intensities for the Ar atom in a strong laser field having a small ellipticity, without any additional phase or polarization measurements. In the vicinity of the Cooper

 ©2016 American Physical Society

minimum in σ_0, the results for β are highly accurate. While the generality of this tool for HHG spectroscopy remains to be established, the accuracy of the results for β obtained here for Ar provide motivation for pursuing the more detailed HHG measurements specified in Refs. [25,26] for retrieving σ_0 and β for arbitrary targets. Provided spin-orbit and fine-structure effects are ignored, the differential cross section (2) for a closed-shell atom such as Ar is exact in *LS* coupling even though it has the same form as for a central potential atomic model [23]. Thus, the parameters $\sigma_0(E)$ and $\beta(E)$ in Eq. (2) are assumed to describe fully correlated ionization from the $3p$ subshell of Ar that can be compared with experimental measurements.

We consider HHG in an elliptically polarized field with electric vector $\mathbf{F}(t) = F/\sqrt{1+\eta^2}[\hat{\mathbf{x}}\cos\omega t + \hat{\mathbf{y}}\eta\sin\omega t]$, where F, ω, and η are the amplitude, frequency, and ellipticity ($-1 \leqslant \eta \leqslant 1$). This parametrization ensures constant field intensity as η is varied, as is realized in our experiment, which employs 30 fs elliptically polarized pulses with up to 2 mJ and $\lambda = 0.78$ μm central wavelength to drive harmonics in Ar. The harmonic yield $Y(E,\eta)$ is measured in an XUV spectrometer comprising a flat-field variable-groove-spacing XUV grating, a z-stack microchannel plate, and a low-noise complementary metal-oxide-semiconductor (CMOS) camera. We vary η by rotating a half-wave plate in front of a quarter-wave plate. The pulse energy is controlled with a half-wave plate and polarizer. Harmonics are measured as a function of focus position relative to the gas jet using a translation stage. To obtain $Y(E,\eta)$ we define a threshold and integrate the remaining image. The normalized HHG yield $\hat{Y}(E,\eta)$, produced by a laser field of intensity 3.8×10^{14} W/cm^2 focused 2.79 mm in front of a gas jet, is given in Fig. 1(a) as a function of harmonic order N and η, where

$$\hat{Y}(E,\eta) = \frac{Y(E,\eta)}{Y(E,\eta=0)}. \tag{3}$$

The experimental results in Fig. 1(a) show that $\hat{Y}(E,\eta)$ varies nonuniformly as η and $E = N\hbar\omega - I_p$ increase. For harmonics $27 \leqslant N \leqslant 37$ (or 27.2 eV $\leqslant E \leqslant$ 43.0 eV),

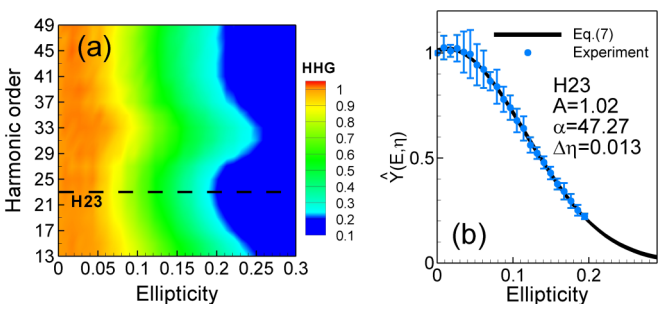

FIG. 1. Normalized HHG yield $\hat{Y}(E,\eta)$ [Eq. (3)] for Ar vs ellipticity η of a $\lambda = 0.78$ μm laser field of intensity 3.8×10^{14} W/cm^2. (a) Results for harmonic orders $13 \leqslant N \leqslant 49$ corresponding to 4.9 eV $\leqslant E \leqslant$ 62.1 eV, where $E = N\hbar\omega - I_p$, $\hbar\omega = 1.59$ eV, and $I_p = 15.8$ eV [cf. Eq. (1)]. Results for $\eta = \pm|\eta|$ are the same [except for a small systematic shift $\Delta\eta \approx 0.01$; cf. Eq. (7)], so only those for $\eta > 0$ are shown. (b) Results for $N = 23$. Blue dots with error bars: experiment; solid line: fit of Eq. (7) to experiment.

$\hat{Y}(E,\eta)$ decreases slowly with increasing η [rather than exponentially, as suggested in Ref. [27] and as found for $N = 23$—see Fig. 1(b)]. This deviation from exponential decrease with increasing η occurs in the region of the Cooper minimum in argon, corresponding to harmonic energies 42.9 eV $\leqslant E_\Omega \leqslant$ 58.8 eV. [Similar features (not shown here) were observed in krypton for harmonic energies 65 eV $\leqslant E_\Omega \leqslant$ 95 eV near the Cooper minimum.]

To retrieve σ_0 and β from $\hat{Y}(E,\eta)$, we employ parametrization of the HHG yield in a field $\mathbf{F}(t)$ having a small ellipticity η that takes into account depletion effects. For an atomic electron having orbital momentum $l = 0$, the parametrization of the HHG yield is similar to Eq. (1), where the dependence of the electronic wave packet $W(E)$ on η and E can be approximated as [28]

$$W(E) \propto e^{-\alpha\eta^2}\sqrt{\frac{E}{E_{\max}-E}}, \quad E < E_{\max}, \tag{4}$$

where $E_{\max} = \mathcal{E}_0(1 - 0.676\eta^2) + 0.324I_p$ is the maximum energy gained by an electron in an elliptically polarized field with small η [cf. Eq. (33) in Ref. [25]], $\mathcal{E}_0 = 3.17U_p$, and $U_p = e^2F^2/(4m\omega^2)$ is the electron quiver energy in the laser field. Also, $\alpha = (F_0/F)(\mathcal{E}_0/I_p)$, where $F_0 = F_{\rm at}(2I_p/E_{\rm at})^{3/2}$ is a reduced atomic field, where $F_{\rm at} = 5.14 \times 10^9$ V/cm and $E_{\rm at} = 27.21$ eV.

The electronic wave packet $W(E)$ in Eq. (4) decreases with increasing η, so only small ellipticities are of interest. This decrease stems from suppression of the ionization step with increasing η for fixed laser intensity. Note that for an initial bound state with $l = 0$, the normalized HHG yield $\hat{Y}(E,\eta)$ is not sensitive to the energy E [28]:

$$\hat{Y}(E,\eta) \propto e^{-\alpha\eta^2} \quad \text{(for an } s \text{ state)}. \tag{5}$$

According to Eq. (2), HHG spectroscopy for $l = 0$ gives the angle-integrated cross section $\sigma_0(E)$ since $\beta \equiv 2$.

For a bound atomic electron with $l > 0$, parametrization of the HHG yield in an elliptically polarized field is more complicated than for an s-state electron since the azimuthal quantum number m (giving the projection of l along the z axis) is not conserved. An initially degenerate (in m) bound state is described by a superposition of substates with different m. For a triply degenerate p state ($l = 1$), the elliptic field forms three different initial substates oriented along the three Cartesian axes: the "$-$" state along the $\hat{x}$ axis (the major polarization axis), the "$+$" state along the $\hat{y}$ axis (the minor polarization axis), and the "0" state along the $\hat{z}$ axis [which defines the propagation direction of the field $\mathbf{F}(t)$] [25,30]. The harmonic yield from the state "0" is suppressed compared to those of the "$+$" and "$-$" states since electron trajectories associated with HHG lie in the polarization plane. Thus we neglect the contribution of the "0" state. Although the states "$-$" and "$+$" are superpositions of the same magnetic substates $\psi_m(\mathbf{r})$ with $m = \pm 1$ [$\psi_\pm \propto (\psi_{+1} \pm \psi_{-1})$], their properties are different [25,31]: (i) In an elliptic field, the "$-$" state decays faster than the "$+$" state, $\Gamma_- > \Gamma_+$, where $\Gamma_\mp$ are ionization rates for the "$-$" and "$+$" states [28]; and (ii) the dipole transition matrix elements $\mathbf{d} = \langle\psi_E|\mathbf{r}|\psi_\mp\rangle$ between the initial ("$-$" or "$+$") state

and the continuum state $|\psi_E\rangle$ have different directions (along the major or minor polarization axes, respectively).

The HHG yield $Y(E,\eta)$ for a p state in an elliptically polarized field is given by the sum of the yields from the initially degenerate "−" and "+" states, each having the factorized form in Eq. (1), with the electronic wave-packet factor $W(E)$ expressed as the product of an ionization factor and a propagation factor (corresponding to the first two steps of the three-step HHG scenario). The wave packets $W_{\mp}(E)$ for the "−" and "+" states differ because their ionization factors differ. The recombination factors in Eq. (1) also differ for the two states, with the "−" state producing harmonics almost linearly polarized along the major polarization axis and the "+" state producing harmonics almost linearly polarized along the minor polarization axis. Thus, for the same kind of classical electron trajectory (which determines the propagation factor), the recombination is determined either by the PRCS for $\theta = 0^\circ$ (for the "−" state) or for $\theta = 90^\circ$ (for the "+" state). The total HHG yield is thus [28]

$$Y(E,\eta) = W(E)[a_-\sigma(E,0^\circ) + a_+\sigma(E,90^\circ)] \tag{6a}$$

$$\propto e^{-\alpha\eta^2}\sigma(E,0^\circ)\left[1 + f(\eta^2)\frac{1-\beta(E)/2}{1+\beta(E)}\right], \tag{6b}$$

where $W(E)$ is given by Eq. (4), $f(\eta^2) \equiv a_+/a_-$, and the coefficients $a_{\mp}$ take into account the difference in ionization factors for the "−" and "+" states (as well as their differences from that for an s state) and also include depletion effects. For small ellipticity, the function $f(\eta^2)$ has an order of magnitude $\propto \eta^2 e^{(\Gamma_- - \Gamma_+)\tau}$ and τ is the laser-pulse duration. Thus depletion effects enhance the second term in Eq. (6). In contrast to Eq. (5) for an s state, Eq. (6b) shows that the normalized HHG yield $\hat{Y}(E,\eta)$ for a p state is energy dependent. It is this energy dependence that allows determination of the asymmetry parameter $\beta(E)$ by measuring the η dependence of $Y(E,\eta)$. For a p-state electron in an alkali or rare-gas atom, the HHG yield in an elliptically polarized field allows the retrieval of both parameters describing the PRCS: For $\eta = 0$, measurements of HHG spectra give the PRCS for $\theta = 0$, while those for a small ellipticity give the asymmetry parameter $\beta(E)$.

The first step for retrieving $\beta(E)$ from the normalized HHG yield $\hat{Y}(E,\eta)$ is to "calibrate" this yield by finding a harmonic for which the dependence of $\hat{Y}(E,\eta)$ on η is close to a Gaussian distribution. From Eq. (6b) it is clear that for an energy E corresponding to such a harmonic $\beta(E) \approx 2$. For Ar the yield of the 23rd harmonic decreases exponentially with η [see the dashed line in Figs. 1(a) and 1(b)]. Owing to experimental uncertainties in the calibration of the laser ellipticity, we fit the η dependence of the HHG yield of the 23rd harmonic by a Gaussian distribution as follows:

$$\hat{Y}^{(\mathrm{G})}(\eta) = Ae^{-\alpha(\eta-\Delta\eta)^2}, \tag{7}$$

where $\Delta\eta$ is a small systematic shift in the zero of η and A is the maximum value of $\hat{Y}^{(\mathrm{G})}(\eta)$ [see Fig. 1(b)].

The second step for retrieving $\beta(E)$ from the normalized HHG yield $\hat{Y}(E,\eta)$ is to remove the exponential term in Eq. (7) from $\hat{Y}(E,\eta)$ for any E. We thus define the auxiliary quantity $\hat{R}$:

$$\hat{R}(E,\eta) = \frac{\hat{Y}(E,\eta)}{\hat{Y}^{(\mathrm{G})}(\eta)} - 1. \tag{8}$$

According to Eq. (6), $\hat{R}(E,\eta)$ is proportional to the ratio of two cross sections, $\sigma(E,90^\circ)/\sigma(E,0^\circ)$, and thus carries information about $\beta(E)$. In Fig. 2(a) we present $\hat{R}(E,\eta)$ as a function of harmonic order N and ellipticity η. This figure shows a hump centered at the 33rd harmonic caused by suppression of the PRCS at 0° by the one at 90° near the Cooper minimum [see Fig. 2(b)], which for Ar corresponds to $E = 36.7 \pm 3$ eV [8,9] (or $E_\Omega = E + I_p = 52.5 \pm 3$ eV).

Experimental data for $\hat{R}(E,\eta)$ at fixed E show that $\hat{R}(E,\eta) \propto \eta^2$ [see Figs. 3(a) and 3(b)]. The third step for retrieving $\beta(E)$ is thus to approximate $\hat{R}(E,\eta)$ as

$$\hat{R}(E,\eta) = B(E)\eta^2, \tag{9}$$

where $B(E)$ is a fitting parameter obtained from the experimental $\hat{R}(E,\eta)$ data. For small η we can approximate the function $f(\eta^2)$ in Eq. (6b) by its leading term, $f(\eta^2) \approx b\eta^2$, where b is a constant. We can then relate $B(E)$ to the asymmetry parameter $\beta(E)$:

$$B(E) = b\frac{1-\beta(E)/2}{1+\beta(E)}, \quad \beta(E) = \frac{1-B(E)/b}{1/2+B(E)/b}. \tag{10}$$

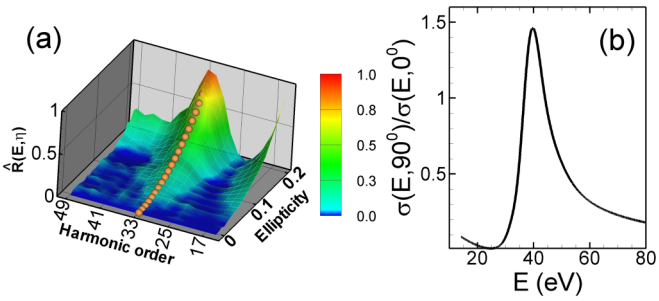

FIG. 2. (a) Experimental results for $\hat{R}(E,\eta)$ [see Eq. (8)] as a function of harmonic order N and ellipticity η. Yellow spheres mark the 33rd harmonic. (b) The ratio $\sigma(E,90^\circ)/\sigma(E,0^\circ) = [1-\beta(E)/2]/[1+\beta(E)]$ [cf. Eq. (2)] as a function of the photoelectron energy E [obtained from theoretical random-phase approximation with exchange (RPAE) results for $\beta(E)$ [32]].

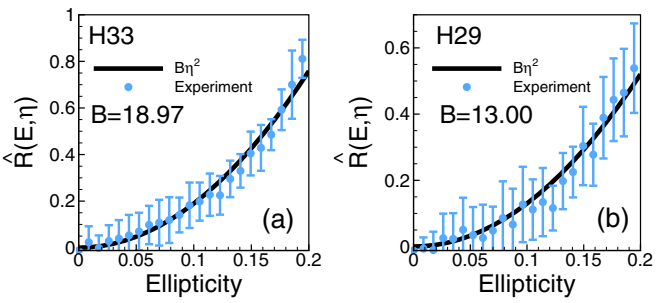

FIG. 3. Ellipticity dependence of $\hat{R}(E,\eta)$ for fixed $E = N\hbar\omega - I_p$ corresponding to the Nth harmonic. Solid lines: $B\eta^2$; circles with error bars: experimental results. (a) $N = 33$ and $B = 18.97$. (b) $N = 29$ and $B = 13.00$.

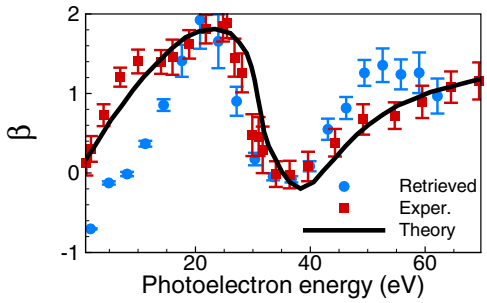

FIG. 4. Energy dependence of the Ar $3p$-subshell photoelectron asymmetry parameter $\beta(E)$. Solid line: RPAE theoretical results [32]; red squares: experimental photoionization measurements [33]; blue circles: present results retrieved from the HHG spectra in Fig. 1(a).

The parameter b can be found by fitting $\beta(E)$ to the value $2-\delta\beta/2$ for the reference harmonic (in our case, H23), for which $\beta \approx 2$. The quantity $\delta\beta$ is a retrieval error, which follows from the experimental error for $B(E)$; the relative magnitude of $\delta\beta$ does not exceed 10%.

In Fig. 4 we present the results for $\beta(E)$ retrieved using the procedure described above. (The self-consistency and the accuracy of this simplified retrieval procedure we discuss in the Supplemental Material [28] using an alternative although more complicated retrieval scheme.) For electron energies over the interval 25 eV $\leqslant E \leqslant$ 50 eV, the $\beta(E)$ results retrieved from the Ar HHG spectra are in excellent agreement with those of both accurate theoretical calculations [32] and experimental photoionization measurements [33]. The discrepancies for energies $E <$ 25 eV may be attributed to (i) inaccuracies in the electronic wave packet used for retrieval (as only the shortest electron trajectory is taken into account, while the contributions of multiple return trajectories are known to be important for low-order harmonics [34,35]), and (ii) the parametrization (6) may fail for low-order harmonics. The discrepancies for energies $E >$ 50 eV are most likely due to the low level of the experimental signal.

Finally, since the PRCS for $\theta = 0^\circ$ can be retrieved from HHG experiments with linear polarization [17] [see Eq. (1)], the angle-integrated PRCS can be obtained as

$$\sigma_0(E) = 4\pi\sigma(E,0^\circ)/[1+\beta(E)]. \tag{11}$$

In summary, we have shown that the limitation of HHG spectroscopy with a linearly polarized field (allowing retrieval of a single photoionization parameter) can be overcome by simple harmonic yield measurements in an elliptically polarized field, in which case complete information on the angular and energy dependence of a target's field-free photoionization cross section can be retrieved. Our experimental and theoretical studies for Ar show also that the normalized HHG yield is sensitive to its electronic structure and exhibits noticeable deviations from the widely accepted Gaussian decrease of the HHG yield with increasing laser ellipticity for harmonics whose energies are near the Cooper minimum in the photoionization cross section. Just as the HHG yield for an elliptically polarized field identifies such features of photoionization cross sections as Cooper minima, HHG spectroscopy with elliptically polarized fields can serve as a tool for scanning other features for various atoms and molecules. The simplicity of the measurement technique should encourage widespread exploration of its generality and its other uses.

The retrieval procedure presented here was supported in part by the Russian Science Foundation through Grant No. 15-12-10033 (M.V.F., T.S.S., A.A.S., and N.V.V.). This research was supported in part by the Chemical Sciences, Geosciences, and Biosciences Division, Office of Basic Energy Sciences, U.S. Department of Energy through Grants No. DE-FG02-86ER13491 (J.T., X.R., and C.A.T.-H.) and No. DE-SC0012198 (E.D.P., K.D.F., and B.P.W.), by NSF-MRI Grant No. 1229672 (X.R.), and by NSF EPSCoR IRR Track II Nebraska-Kansas Collaborative Research Awards No. 1430519 (A.F.S.) and No. 1430493 (C.A.T.-H.). K.D.F. acknowledges a Louisiana Board of Regents Fellowship.

[1] J. Itatani, J. Levesque, D. Zeidler, H. Niikura, H. Pépin, J. C. Kieffer, P. B. Corkum, and D. M. Villeneuve, Tomographic imaging of molecular orbitals, Nature (London) **432**, 867 (2004).

[2] A. Föhlisch, P. Feulner, F. Hennies, A. Fink, D. Menzel, D. Sanchez-Portal, P. M. Echenique, and W. Wurth, Direct observation of electron dynamics in the attosecond domain, Nature (London) **436**, 373 (2005).

[3] P. B. Corkum and F. Krausz, Attosecond science, Nat. Phys. **3**, 381 (2007).

[4] F. Krausz and M. Ivanov, Attosecond physics, Rev. Mod. Phys. **81**, 163 (2009).

[5] S. Haessler, J. Caillat, W. Boutu, C. Giovanetti-Teixeira, T. Ruchon, T. Auguste, Z. Diveki, P. Breger, A. Maquet, B. Carré, R. Taïeb, and P. Salières, Attosecond imaging of molecular electronic wavepackets, Nat. Phys. **6**, 200 (2010).

[6] E. Goulielmakis, Z.-H. Loh, A. Wirth, R. Santra, N. Rohringer, V. S. Yakovlev, S. Zherebtsov, T. Pfeifer, A. M. Azzeer, M. F. Kling, S. R. Leone, and F. Krausz, Real-time observation of valence electron motion, Nature (London) **466**, 739 (2010).

[7] J. Cooper and R. N. Zare, Photoelectron Angular Distributions, in *Lectures in Theoretical Physics*, Vol. XI (Gordon and Breach, New York, 1969), pp. 317–337.

[8] A. F. Starace, Theory of Atomic Photoionization, in *Handbuch der Physik*, edited by W. Mehlhorn (Springer, Berlin, 1982), Vol. XXXI, pp. 1–121.

[9] M. Ya. Amusia, *Atomic Photoeffect* (Plenum, New York, 1990).

[10] H. J. Wörner, H. Niikura, J. B. Bertrand, P. B. Corkum, and D. M. Villeneuve, Observation of Electronic Structure Minima in High-Harmonic Generation, Phys. Rev. Lett. **102**, 103901 (2009).

[11] A. D. Shiner, B. E. Schmidt, C. Trallero-Herrero, H. J. Wörner, S. Patchkovskii, P. B. Corkum, J.-C. Kieffer, F. Légaré, and D. M. Villeneuve, Probing collective multi-electron dynamics in xenon with high-harmonic spectroscopy, Nat. Phys. **7**, 464 (2011).

[12] J. B. Bertrand, H. J. Wörner, P. Hockett, D. M. Villeneuve, and P. B. Corkum, Revealing the Cooper Minimum of N_2 by Molecular Frame High-Harmonic Spectroscopy, Phys. Rev. Lett. **109**, 143001 (2012).

[13] M. C. H. Wong, A.-T. Le, A. F. Alharbi, A. E. Boguslavskiy, R. R. Lucchese, J.-P. Brichta, C. D. Lin, and V. R. Bhardwaj, High Harmonic Spectroscopy of the Cooper Minimum in Molecules, Phys. Rev. Lett. **110**, 033006 (2013).

[14] A. D. Shiner, B. E. Schmidt, C. Trallero-Herrero, P. B. Corkum, J.-C. Kieffer, F. Légaré, and D. M. Villeneuve, Observation of Cooper minimum in krypton using high harmonic spectroscopy, J. Phys. B **45**, 074010 (2012).

[15] P. B. Corkum, Plasma Perspective on Strong Field Multiphoton Ionization, Phys. Rev. Lett. **71**, 1994 (1993).

[16] K. C. Kulander, K. J. Schafer, and J. L. Krause, Dynamics of short-pulse excitation, ionization and harmonic conversion, in *Super-Intense Laser-Atom Physics*, edited by A. L'Huillier, B. Piraux, and K. Rzazewski, NATO Science Series B Vol. 316 (Springer, New York, 1993), pp. 95–110.

[17] T. Morishita, A.-T. Le, Z. Chen, and C. D. Lin, Accurate Retrieval of Structural Information from Laser-Induced Photoelectron and High-Order Harmonic Spectra by Few-Cycle Laser Pulses, Phys. Rev. Lett. **100**, 013903 (2008).

[18] A.-T. Le, T. Morishita, and C. D. Lin, Extraction of the species-dependent dipole amplitude and phase from high-order harmonic spectra in rare-gas atoms, Phys. Rev. A **78**, 023814 (2008).

[19] M. V. Frolov, N. L. Manakov, T. S. Sarantseva, and A. F. Starace, Analytic confirmation that the factorized formula for harmonic generation involves the exact photorecombination cross section, Phys. Rev. A **83**, 043416 (2011).

[20] M. V. Frolov, N. L. Manakov, T. S. Sarantseva, M. Yu. Emelin, M. Yu. Ryabikin, and A. F. Starace, Analytic Description of the High-Energy Plateau in Harmonic Generation by Atoms: Can the Harmonic Power Increase with Increasing Laser Wavelengths? Phys. Rev. Lett. **102**, 243901 (2009).

[21] M. V. Frolov, N. L. Manakov, and A. F. Starace, Potential barrier effects in high-order harmonic generation by transition-metal ions, Phys. Rev. A **82**, 023424 (2010).

[22] J. A. R. Samson and A. F. Starace, Effect of elliptically polarized light on the angular distribution of photelectrons, J. Phys. B **8**, 1806 (1975); see also the Corrigendum, J. Phys. B **12**, 3993 (1979).

[23] S. T. Manson and A. F. Starace, Photoelectron angular distributions: energy dependence for s subshells, Rev. Mod. Phys. **54**, 389 (1982). See the general discussion of angular distributions in Secs. II and III.

[24] N. L. Manakov, S. I. Marmo, and A. V. Meremianin, A new technique in the theory of angular distributions in atomic processes: the angular distribution of photoelectrons in single and double photoionization, J. Phys. B **29**, 2711 (1996).

[25] M. V. Frolov, N. L. Manakov, T. S. Sarantseva, and A. F. Starace, High-order-harmonic-generation spectroscopy with an elliptically polarized laser field, Phys. Rev. A **86**, 063406 (2012).

[26] T. S. Sarantseva, M. V. Frolov, N. L. Manakov, M. Yu. Ivanov, and A. F. Starace, Harmonic generation spectroscopy with a two-colour laser field having orthogonal linear polarizations, J. Phys. B **46**, 231001 (2013).

[27] M. Möller, Y. Cheng, S. D. Khan, B. Zhao, K. Zhao, M. Chini, G. G. Paulus, and Z. Chang, Dependence of high-order-harmonic-generation yield on driving-laser ellipticity, Phys. Rev. A **86**, 011401(R) (2012).

[28] See Supplemental Material at http://link.aps.org/supplemental/10.1103/PhysRevA.93.031403, which includes Ref. [29], for a derivation of Eqs. (4)–(6), a justification of the relation $\Gamma_- > \Gamma_+$, and a discussion of the generality and accuracy of our retrieval procedure for $\beta(E)$.

[29] B. M. Smirnov and M. I. Chibisov, The breaking up of atomic particles by an electric field and by electron collisions, Zh. Eksp. Teor. Fiz. **49**, 841 (1965) [Sov. Phys. JETP **22**, 585 (1966)].

[30] M. V. Frolov, N. L. Manakov, and A. F. Starace, Effective-range theory for an electron in a short-range potential and a laser field, Phys. Rev. A **78**, 063418 (2008).

[31] I. Barth and O. Smirnova, Nonadiabatic tunneling in cicularly polarized laser fields: Physical picture and calculations, Phys. Rev. A **84**, 063415 (2011).

[32] M. Ya. Amusia, N. A. Cherepkov, and L. V. Chernysheva, Angular distribution of photoelectrons with many-electron correlations, Phys. Lett. A **40**, 15 (1972).

[33] R. G. Houlgate, J. B. West, K. Codling, and G. V. Marr, The angular distribution of the $3p$ electrons and the partial cross section of the $3s$ electrons of argon from threshold to 70 eV, J. Electron Spectrosc. Relat. Phenom. **9**, 205 (1976).

[34] D. B. Milošević and W. Becker, Role of long quantum orbits in high-order harmonic generation, Phys. Rev. A **66**, 063417 (2002).

[35] M. V. Frolov, N. L. Manakov, W.-H. Xiong, L.-Y. Peng, J. Burgdörfer, and A. F. Starace, Scaling laws for high-order harmonic generation with midinfrared laser pulses, Phys. Rev. A **92**, 023409 (2015).